Contrib Mineral Petrol (2009) 157:267–279
DOI 10.1007/s00410-008-0333-x

ORIGINAL PAPER

Do extrusion ages reflect magma generation processes at depth? An example from the Neogene Volcanic Province of SE Spain

Bernardo Cesare · Daniela Rubatto · María Teresa Gómez-Pugnaire

Received: 24 April 2008 / Accepted: 25 July 2008 / Published online: 21 August 2008

Abstract The high-K calc-alkaline volcanic rocks along the Neogene Volcanic Province of SE Spain represent crustal anatectic melts mixed with mantle components during the opening of the Alborán Sea. Partially melted metapelitic enclaves, along with the geochemical signature, provide evidence of their crustal source. U–Pb SHRIMP geochronology on monazite and zircon from enclaves and their hosting lavas in the localities of El Hoyazo, Mazarrón and Mar Menor reveals variable delays between the melting at depth and the eruption of the volcanics. These data indicate that: (1) the most important event of anatexis in the Neogene spanned at least the 3 m.y. interval between 12 and 9 Ma; (2) there is no trend in age of crustal melting; and (3) the delay between magma generation and extrusion varies from more than 3 m.y. at El Hoyazo to ~0.5 m.y. and possibly 2.5 m.y. at Mar Menor, with no significant delay measurable at Mazarrón. The variable time delay between anatexis and lava extrusion indicates that radiometric ages of volcanics may provide misleading information on the timing of magma genesis occurring at depth. This highlights the pitfall of basing detailed geodynamic models on volcanic extrusion ages alone.

Keywords Anatexis · Geochronology · Monazite · SHRIMP · Southern Spain · Volcanism · Zircon

Communicated by J. Hoefs.

Electronic supplementary material The online version of this article (doi:10.1007/s00410-008-0333-x) contains supplementary material, which is available to authorized users.

B. Cesare (✉)
Dipartimento di Geoscienze, Università di Padova, Via Giotto 1, 35137 Padua, Italy
e-mail: bernardo.cesare@unipd.it

B. Cesare
C.N.R. Istituto di Geoscienze e Georisorse, Corso Garibaldi, 37, 35137 Padua, Italy

D. Rubatto
Research School of Earth Sciences, The Australian National University, Canberra, ACT 0200, Australia

M. T. Gómez-Pugnaire
Departamento de Mineralogía y Petrología, Facultad de Ciencias, Universidad de Granada, Fuentenueva s/n, 18002 Granada, Spain

M. T. Gómez-Pugnaire
Instituto Andaluz de Ciencias de la Tierra (CSIC), Facultad de Ciencias, Universidad de Granada, Fuentenueva s/n, 18002 Granada, Spain

The problem

Partial melting of the metasedimentary crust occurs in areas of anomalously high temperature and produces peraluminous felsic magmas, which generally crystallize at depth as leucogranitic plutons (e.g. Clemens 2003). More rarely, these viscous and relatively cold magmas may rise and extrude to the Earth's surface, often with explosive eruptions (e.g. Pallister et al. 1992). The fate of anatectic melts and the timescales in which they form, crystallize, and erupt may be extremely variable and difficult to constrain. This depends on the geodynamic setting (the thermal regime in the lithosphere) and the structural setting of the lithosphere (the stress field and the location of anisotropies and fracture systems), as well as on the chemical and rheological properties of the magma (viscosity and density contrast with respect to country rocks; Clemens and Droop 1998; Petford et al. 2000). Further complexity is provided by the difficulty of defining a clear petrogenetic link between anatectic melts and their source rocks (e.g. Vernon 2007). As a result, it is not uncommon to assume the products of crustal melting—felsic lavas—as reflecting, for example in time evolution, the history of their source rocks (e.g. Zeck et al. 2000; Christiansen et al. 2002; Duggen et al. 2004). However, this assumption may not always be valid, as the age of extrusion needs not necessarily be the same as that of magma formation.

In the Neogene Volcanic Province (NVP) of SE Spain, for example, various rock types with different geochemical affinities occur, including tholeiitic basalts, calc-alkaline basaltic andesites to rhyodacites, strongly peraluminous high-K calc-alkaline andesites and dacites, shoshonitic rocks, lamproites, and alkali basalts (e.g. Benito et al. 1999). Based on available geochemical and geochronological data, the volcanism in the NVP has been interpreted according to various, often contrasting, petrogenetic models (see Duggen et al. 2008 for a recent discussion extended to the whole Alborán Basin), which reflect the uncertainties in the geodynamic scenario during the Neogene (e.g. Gueguen et al. 1998 vs. Duggen et al. 2005). In these models, ages for NVP volcanics have been used to infer time–space relationships. Benito et al. (1999) propose a NE-oriented geochemical, petrological and age polarity zonation, with progressively younger volcanic ages; Gill et al. (2004) mention a W-migrating volcanic front above a retreating subduction zone; Duggen et al. (2005) model a westwards movement of the subduction- to intraplate-type magmatic transition. The time frames of all these models are based on the age of volcanics, but one major uncertainty is whether volcanism is contemporaneous with the production of magmas at depth, i.e. with the process that has the real significance for geodynamic reconstructions.

In this study we show the time relationships between crustal melting and extrusion of lavas in the NVP, focusing our attention on the high-K calc-alkaline (HKCA) products, which are dominated by an anatectic component (Benito et al. 1999; Turner et al. 1999; Gill et al. 2004). Time constraints were produced by SHRIMP ion microprobe dating of zircon and monazite contained in lavas and in the hosted crustal enclaves. These enclaves show evidence of partial melting (e.g. Acosta-Vigil et al. 2007; Cesare et al. 2007) and have been considered representative of the source of the crustal component of the lavas (Zeck 1970; Cesare et al. 1997). Although HKCA lavas show evidence of mixing with mantle-derived magmas (see below), and therefore do not have a uniquely anatectic origin, this does weaken the approach of this work, that is aimed at providing age constraints on crustal anatexis and eruption of crustally-derived magmas. The petrological background for this research comes mostly from the extensive study of anatectic enclaves from the dacite of El Hoyazo (Cesare 2008 and references therein). For this locality, the interpretation of enclaves as restites and the peritectic origin of garnet have been recently challenged by Vernon (2007), mainly on the basis of his model for the formation of melt inclusions in garnet. While, as discussed theoretically by Cesare (2008), such model is unlikely in general, in this paper we demonstrate that it is not applicable to the specific case study of El Hoyazo, where we have been able to date the monazite included in garnet, and to show that garnet must have grown in the presence of melt.

Owing to the young ages (9–12 Ma), which are associated to low age uncertainties (<250 k.y.), the NVP is an ideal case study for this kind of approach. Geochronology demonstrates that the age of crustal melting recorded in the enclaves does not necessarily correspond to that of the erupting lavas. In addition to its general implications, this work provides further constraints on the magmatic history of the extensional margin of the Alborán Domain, with the first U–Pb data on volcanics from Mar Menor, and a new model for the chronology of crustal melting in the area.

Geological setting

The Alborán Domain (Fig. 1), in the Betic-Rif orogen in the western Mediterranean, is a fragment of a collisional mountain belt that underwent a late orogenic extension of Miocene age (García-Dueñas et al. 1992; Platt et al. 2003). The extension and the subsequent crustal thinning (between 14 and 22 km, Torné et al. 2000) were accompanied by volcanism of calc-alkaline (mostly andesites, Fernández-Soler 1996), high-K calc-alkaline (HKCA), and minor shoshonitic compositions (Zeck et al. 1998; Turner et al. 1999 and references therein). Volcanism continued after extension, with limited high-K lavas (lamproites, Venturelli et al. 1984) and intra-plate alkali basalts. These volcanic rocks form the NVP (Fig. 1, López-Ruíz and Rodríguez-Badiola 1980) that extends for about 500 km following a NE-SW trend from N Africa to SE Spain through the Alborán Sea (Comas et al. 1996).

This work focuses on the HKCA lavas represented by peraluminous garnet- and cordierite-bearing dacites and SiO_2-rich andesites. In the Internal Betics, the HKCA volcanic rocks occur in scattered volcanic centres depicting an arc parallel to the coast line from Carboneras to Mar Menor (Fig. 1). The volcanism appears to be controlled by the Carboneras and Palomares faults, a strike-slip system operating under compressional tectonics in the last 9 Ma (Gracia et al. 2006). These faults displaced the eastern part of the original volcanic province towards the N and produced the present-day arc of the coast line (De Larouziere and Ott d'Estevou 1990). Extrusion of magmas was

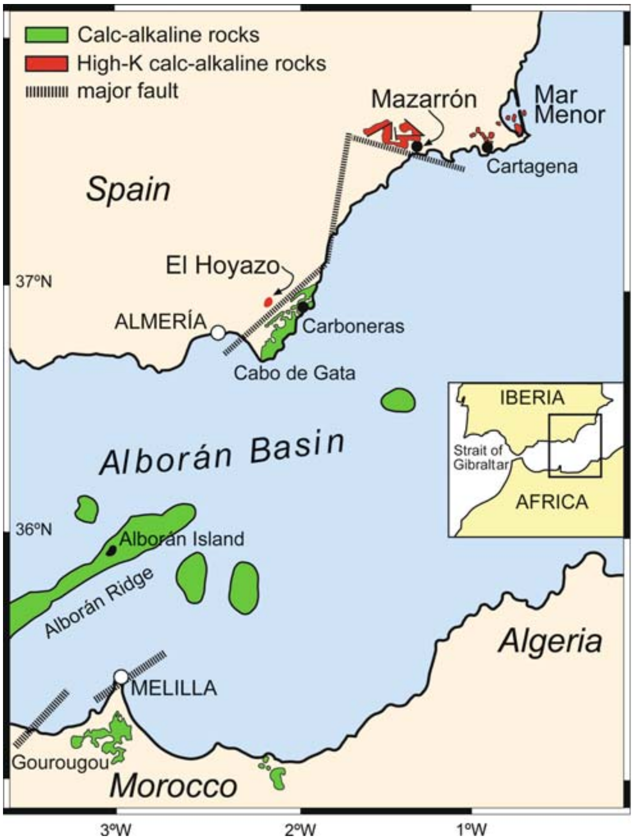

Fig. 1 Simplified sketch of the Alborán Domain in the western Mediterranean, with location of the main outcrops of NVP volcanic rocks, and of the studied high-K calc-alkaline rocks

favoured by local extension through normal faults, as can be observed in the Mazarrón area or, less markedly, in the volcanic trend from Cartagena to Mar Menor.

In the NVP, the HKCA lavas are the most acidic volcanic rock suite, and contain abundant partially melted metapelitic enclaves, which are interpreted as restites after anatexis of crustal protoliths (Zeck 1992; Cesare et al. 1997; Cesare 2008). In turn, the lavas are considered the accompanying anatectic melts, mixed with mantle-derived magmas whose precise nature is still uncertain (Zeck 1992; Benito et al. 1999; Duggen et al. 2005; Fernandez-Soler et al. 2007).

The enclaves in the volcanic rocks of the NVP have been extensively studied in the last decade (Cesare et al. 1997, 2002, 2003a, b, c, 2005, 2007; Cesare and Maineri 1999; Cesare and Gomez-Pugnaire 2001; Cesare 2000, 2008; Alvarez-Valero et al. 2005, 2007; Acosta-Vigil et al. 2007; Alvarez-Valero and Kriegsman 2007; Ferri et al. 2007) and the reader may refer to these works for the details of their geology, petrology, mineralogy, geochronology and rock-physics. In particular, the restitic enclaves consist of Sil-Crd-Spl-Ilm-Grt-Gr-glass ± Kfs ± Bt (mineral abbreviations according to Kretz 1983) at Mar Menor (Álvarez-Valero and Kriegsman 2008), of Crd-Sil-Grt-Bt-Pl-Kfs-Ilm-Gr-glass at Mazarrón (Cesare et al. 2003b, c) and of Crd-Spl-Sil-Bt-Kfs-Pl-Gr-glass at El Hoyazo (Cesare et al. 1997; Alvarez-Valero et al. 2005). In the latter locality, thermobarometric estimates indicate equilibration temperature of 850 ± 50°C and pressure of 5–7 kbar. Evidence of partial melting is provided by abundant glass, still well preserved and occurring throughout the enclaves. The most important mode of occurrence of glass is as inclusions in major minerals (e.g. garnet, plagioclase, cordierite, ilmenite, andalusite (Cesare et al. 2003c; Acosta-Vigil et al. 2007), as well as in monazite and zircon (Cesare et al. 2003b).

Previous U–Pb SHRIMP geochronology on the HKCA volcanics of the NVP is limited to two studies. The first one carried out age determination on zircon from the Grt-Crd-bearing dacite of El Hoyazo (Zeck and Williams 2002), which provided an age of extrusion of 6.33 ± 0.15 Ma. In the same work the inherited cores of zircons from the anatectic enclaves were also dated systematically. The second is the dating of zircon and monazite from enclaves from El Hoyazo and from enclaves and host lava from Mazarrón (Cesare et al. 2003b), extensively referred to below. Before SHRIMP chronology, lavas were dated by Ar/Ar on biotite by Turner et al. (1999) who obtained ages of 6.2 ± 0.4 Ma at El Hoyazo, and of 8.8 ± 0.2 and 8.9 ± 0.6 Ma at Mazarrón. Volcanics from east of Mazarrón were also dated at 6.8 and 7.2 Ma by K/Ar on whole rock by Bellon et al. (1983). More recently, HKCA lavas from El Hoyazo and Mar Menor were dated by laser Ar/Ar on biotite by Duggen et al. (2004) who obtained ages of 6.57 ± 0.04 and 18.5 ± 1.6, respectively.

The uniqueness of these rocks for the understanding of crustal melting and the behaviour of migmatites is given by the combination of their extremely rapid cooling and deep crustal provenance. In this perspective, the definition of "erupted migmatites" attributed by Zeck (1970) to the enclaves of El Hoyazo appears appropriate.

For the following discussion and interpretation of results it is important to outline: that HKCA lavas are the only outcropping volcanics in the NVP which contain crustal enclaves; that the crustal fragments consist of two types of anatectic rocks, accounting for the majority (>60 vol %; Zeck 1970) of foreign material; that the amount of crustal material (enclaves down to single crystals resulting from their disaggregation) is very abundant (10–15 vol %; Zeck 1992) and homogeneously distributed throughout the volcanic outcrop; that in the NVP there are no occurrences of peraluminous intermediate to felsic HKCA rocks that are devoid of partially melted crustal material. Although they do not represent a proof of the restitic origin of crustal enclaves in the HKCA lavas, these features nonetheless suggest a very close relationship between the two rock types.

Samples

The samples investigated are two lava-enclave pairs from Mar Menor (samples ICL and IC10 from Isla del Ciervo and IR1 and IR17 from Isla Redondela), one enclave from Mazarrón (PF-MA5), and two enclaves from El Hoyazo (HZ14 and HO50). Along with previous SHRIMP studies of rocks from El Hoyazo and Mazarrón (Zeck and Williams 2002; Cesare et al. 2003b) these samples provide a comprehensive U–Pb geochronological record of the HKCA volcanics of the NVP.

Enclave IR17 from Mar Menor (Isla Redondela) is a medium-grained foliated rock consisting of sillimanite, cordierite, garnet, spinel, feldspars, ilmenite, graphite and glass. A syn-anatectic foliation (e.g. Cesare et al. 1997) is present and marked by sillimanite anastomosing around garnet with melt inclusions (Fig. 2). This foliation is then overgrown statically by cordierite and spinel. Cordierite replaces garnet pseudomorphically and contains glass inclusions (Fig. 3). Biotite occurs only as inclusions in garnet, indicating that the enclaves reached the P–T conditions for biotite melting. Melt inclusions are observed also within apatite.

Sample IC10 from Mar Menor (Isla del Ciervo) is a fine-grained, sillimanite-rich, foliated enclave consisting of cordierite, fibrolitic sillimanite, spinel, ilmenite, glass and rare garnet. The rock is rich in cordierite, sillimanite and interstitial glass, whereas garnet and biotite occur as rare resorbed relicts. Feldspars are absent. Melt inclusions are present in cordierite, apatite and monazite (Fig. 4).

Enclave PF-MA5 from Mazarrón is a medium-grained gneissic rock consisting of plagioclase, K-feldspar, cordierite, garnet, biotite, sillimanite, ilmenite, graphite and glass. Garnet porphyroblasts >5 mm are rich in inclusions of fibrolite, and display resorption textures. Plagioclase is abundant and contains inclusions of graphite and glass. Crystals of biotite are also frequent, in places with resorbed aspect and enclosed in feldspars. Graphite is abundant, whereas cordierite is rare. Similarly to other enclaves, glass inclusions are present in monazite (Fig. 5).

Enclave HZ14 from El Hoyazo is a typical fine-grained Spl-Crd-rock (according to the definition of Zeck 1970) containing hercynitic spinel, cordierite, fibrolitic sillimanite, biotite, plagioclase, glass and graphite. The average grain size is <1 mm, and the rock is characterised by a well-developed folded foliation outlined by biotite and fibrolite, which is overgrown by postkinematic, euhedral spinel porphyroblasts (Fig. 6). Glass is present as melt inclusions in all phases, and intergrown with fibrolite in the matrix. Garnet is absent in this sample, probably by complete replacement by Spl + Crd.

Sample HO50 is a Bt-Grt-Sil enclave, the most common type at El Hoyazo. These rocks usually contain garnet with inclusions of glass (melt inclusions), interpreted as evidence that garnet is a peritectic phase formed during partial melting of a metapelitic protolith (Cesare and Maineri 1999). Two similar samples (HO02 and HO33) were dated by Cesare et al. (2003b) and overlapped in age at 9.63 ± 0.26 for zircon and 9.74 ± 0.21 for monazite. Recently the peritectic origin of garnet was questioned by Vernon (2007), and thus we extracted several garnet porphyroblasts from HO50 to date monazite and zircon included in them. In fact, the age of inclusions would in turn constrain the age of garnet growth and provide a test for its peritectic nature. Garnets of 4–6 mm in diametre were mounted in epoxy and cut close to their equatorial section. They include zircons with thin euhedral overgrowths marked by an alignment of tiny melt inclusions (Fig. 7), similar to those dated in other samples from El Hoyazo (Cesare et al. 2003b). The garnet crystals also contain monazite, often with melt inclusions. Zircon and monazite inclusions occur throughout garnet crystals from sample HO50, without a preferred microstructural location.

The studied lavas are one Grt-Crd-bearing dacite from Mazarrón (Cesare et al. 2003b) and two high-SiO_2 Crd-bearing andesites from Mar Menor. The bulk composition of these samples (Table 1), is similar to those reported for other HKCA lavas by Benito et al. (1999) for Mazarrón and by Duggen et al. (2004) for Mar Menor. The samples are peraluminous, as expected for lavas with an important crustal component. Compared with the rhyolitic composition of primary anatectic melts occurring as glass inclusions in minerals of the enclaves (Acosta-Vigil et al. 2007; Cesare et al. 2003c), the lavas are more mafic. This mafic signature attests for both mixing with mantle magmas and contamination of the lavas with restitic material rich in garnet, sillimanite, cordierite and hercynite.

Methods

Whole-rock major and trace element compositions were obtained by X-ray fluorescence (XRF) with the Philips PW 2400 spectrometer of C.N.R.—I.G.G., Padova.

Except for the mount of garnet porphyroblasts from sample HO50, zircon and monazite for U–Th–Pb analysis were prepared as mineral separates mounted in epoxy and polished down to expose the grain centres. Cathodoluminescence (CL) and back-scattered electron (BSE) images of zircon and monazite were carried out at the Electron Microscope Unit, Australian National University. The CL investigation was performed with a HITACHI S2250-N scanning electron microscope working at 15 kV, $\sim$60 μA and $\sim$20 mm working distance. BSE images of monazite were obtained with a Cambridge S360 scanning electron microscope using a

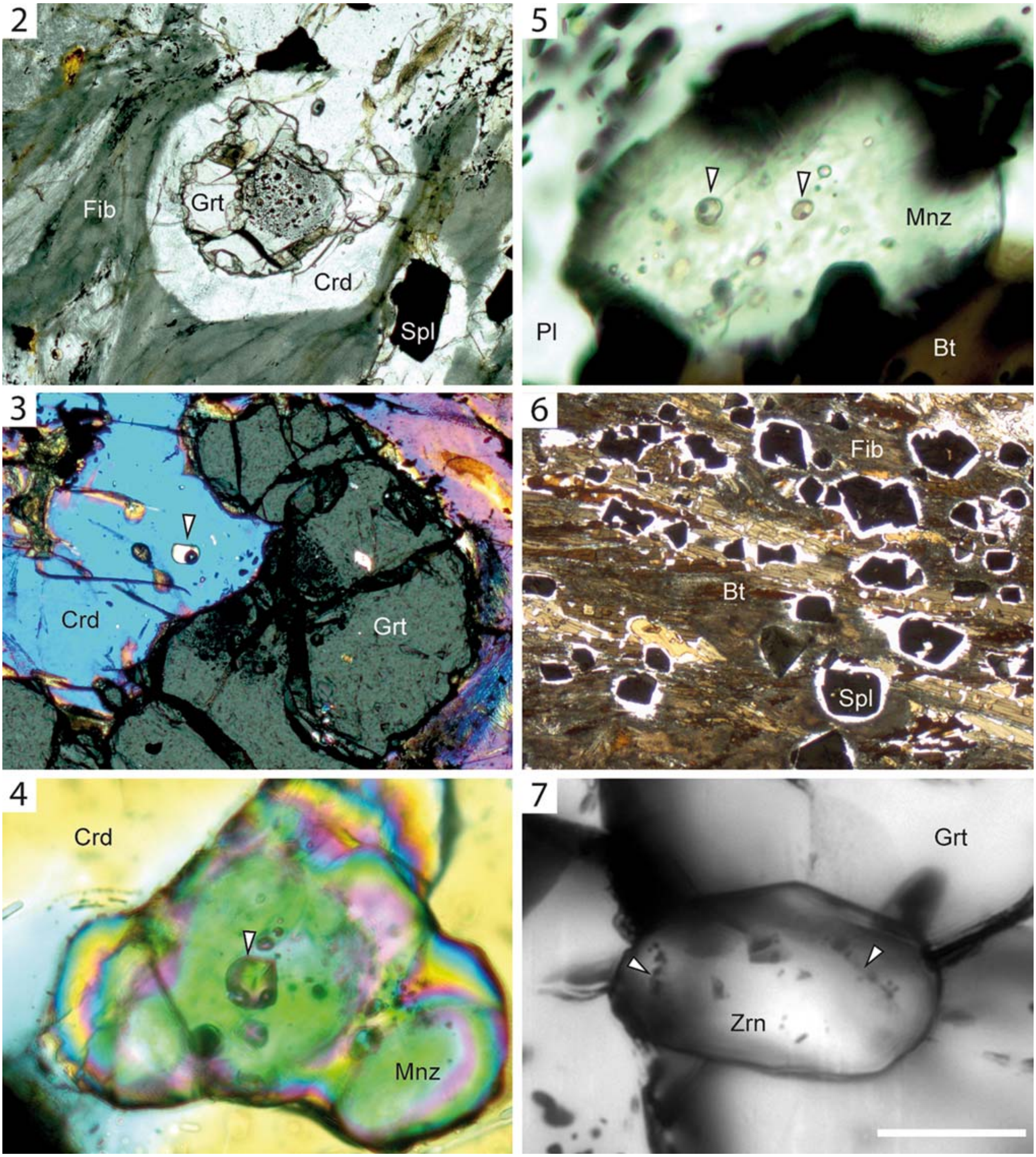

Figs. 2–7 **Fig. 2** Fibrolite-rich foliation wrapping around a crystal of garnet, partly pseudomorphed by cordierite, in sample IR17. Plane-polarised light, width of view: 8 mm. **Fig. 3** Cordierite (*blue*) with one large glass inclusion (*white, with shrinkage bubble*) replacing garnet (*gray*) in sample IR17. The core of garnet contains abundant, minute inclusions of glass. Partly crossed polarizers, width of view: 4 mm. **Fig. 4** Primary glass inclusions (*arrow*) in monazite (Mnz) included in cordierite (Crd) from sample IC10, attesting to the growth of monazite in the presence of melt, i.e. during partial melting of the enclave. Width of view: 230 µm. **Fig. 5** Glass inclusions (*arrows*) in monazite from sample PF-MA 5. Plane-polarised light, width of view: 100 µm. **Fig. 6** Hercynite-rich spinel, with white coronae of K-feldspar statically overgrowing the biotite-fibrolite-rich matrix of sample HZ14. Plane-polarised light, width of view: 8 mm. **Fig. 7** Crystal of zircon included in garnet from sample HO50. The boundary between inherited core and euhedral overgrowths is defined by small inclusions. Euhedral overgrowths are well developed in the upper part (*arrow*). Plane-polarised light, scalebar: 25 µm

Table 1 Whole-rock major and trace element compositions of the dated lava samples

	Mar Menor 1	Mar Menor 2	Mazarrón
SiO_2	60.43	60.23	62.88
TiO_2	0.66	0.64	0.60
Al_2O_3	15.63	15.50	15.48
Fe_2O_3	6.11	6.12	4.62
MnO	0.09	0.09	0.07
MgO	4.31	4.29	2.15
CaO	5.01	5.00	2.54
Na_2O	1.67	1.90	2.21
K_2O	2.17	2.20	4.02
P_2O_5	0.14	0.15	0.32
L.O.I.	3.34	3.09	4.65
Total	99.56	99.20	99.55
Sc	18	18	17
V	134	136	99
Cr	283	234	108
Co	21	19	12
Ni	267	60	26
Cu	12	7	8
Zn	54	50	53
Ga	16	17	17
Rb	110	116	211
Sr	152	163	464
Y	24	27	27
Zr	140	138	236
Nb	10	10	17
Ba	312	333	1,017
La	41	27	54
Ce	54	48	137
Nd	16	10	<10
Pb	<5	<5	22
Th	<3	<3	37
U	4	3	14
ASI*	1.10	1.06	1.23

**ASI* aluminium saturation index

voltage of 20 kV, current of ~2 nA and a working distance of ~20 mm.

U–Th–Pb analyses were performed using a sensitive, high-resolution ion microprobe (SHRIMP II) at the Research School of Earth Sciences (RSES). Instrumental conditions and data acquisition were generally as described by Williams (1998). The data were collected in sets of seven or six scans throughout the masses. The measured $^{206}Pb/^{238}U$ ratio was corrected using reference zircon (417 Ma, Black et al. 2003) and monazite (425 Ma, Aleinikoff et al. 2007). Zircon and monazite data were corrected for common Pb on the basis of the measured $^{207}Pb/^{206}Pb$ ratios as described in Williams (1998). Age calculation was done using the software Isoplot/Ex (Ludwig 2003) and assuming the common Pb composition predicted by Stacey and Kramers (1975). Whenever there was sufficient spread in the total $^{207}Pb/^{206}Pb$ versus $^{238}U/^{206}Pb$, free intercepts were also calculated and the ages are always identical within the limits of uncertainty. U–Pb data were collected over a number of analytical sessions in the same laboratory and using the same ion microprobe and zircon and monazite standards. The different analytical sessions have comparable calibration errors between 1.5 and 2.5% (2σ). For these reasons data from different samples are directly comparable. Results are reported in Table 2 (available as electronic supplementary material, ESM) and in Fig. 8, where average ages are quoted at 95% confidence level (Cl).

Results

At Mar Menor, monazite with glass inclusions were dated from two crustal enclaves, which contain only tiny zircons showing metamorphic overgrowths too small for dating. (Fig. 8a, b). In sample IR17, monazite displays high-BSE cores with internal zoning, which are truncated by homogeneous, low-BSE rims. Despite this chemical zoning, no age difference was detected between the two domains and the 15 analyses define a single population with an age of 10.05 ± 0.17 Ma. In sample IC10, monazite displays a similar core-rim zoning as in IR17. In this sample however, monazite cores and rims are distinct in age with 11.94 ± 0.19 Ma and at 10.02 ± 0.22 Ma, respectively. A few analyses yielded intermediate apparent ages, which probably reflect physical mixing of the two small domains.

The two lava samples of Mar Menor do not contain monazite, but have abundant euhedral, double terminated zircon crystals. The zircons have oscillatory zoning with apparent cores. Dating was targeting crystallization and thus concentrated on the external growth zones, which yielded ages that overlap within error at 9.48 ± 0.25 Ma for sample ICL and 9.63 ± 0.23 Ma for sample IR1.

At Mazarrón the enclave contains both monazite and zircon, but the latter are composed of detrital cores with metamorphic overgrowth too small (<5–10 μm) to be dated. Monazite displays dramatic internal zoning, generally with a progressive decrease in BSE-emission from core to rim. Cores can also display a butterfly-type zoning. Despite the zoning, U–Pb analyses of cores and rims are

Fig. 8 Geochronological data. Tera-Wasserburg plots of radiogenic ratios uncorrected for common Pb. Age regressions are to the common Pb composition predicted by the model of Stacey and Kramers (1975). Average ages are at 95% Cl. *Insets* represent back-scattered electron (monazites) or cathodoluminescence (zircon) images of representative crystals with the SHRIMP pits marked ▶

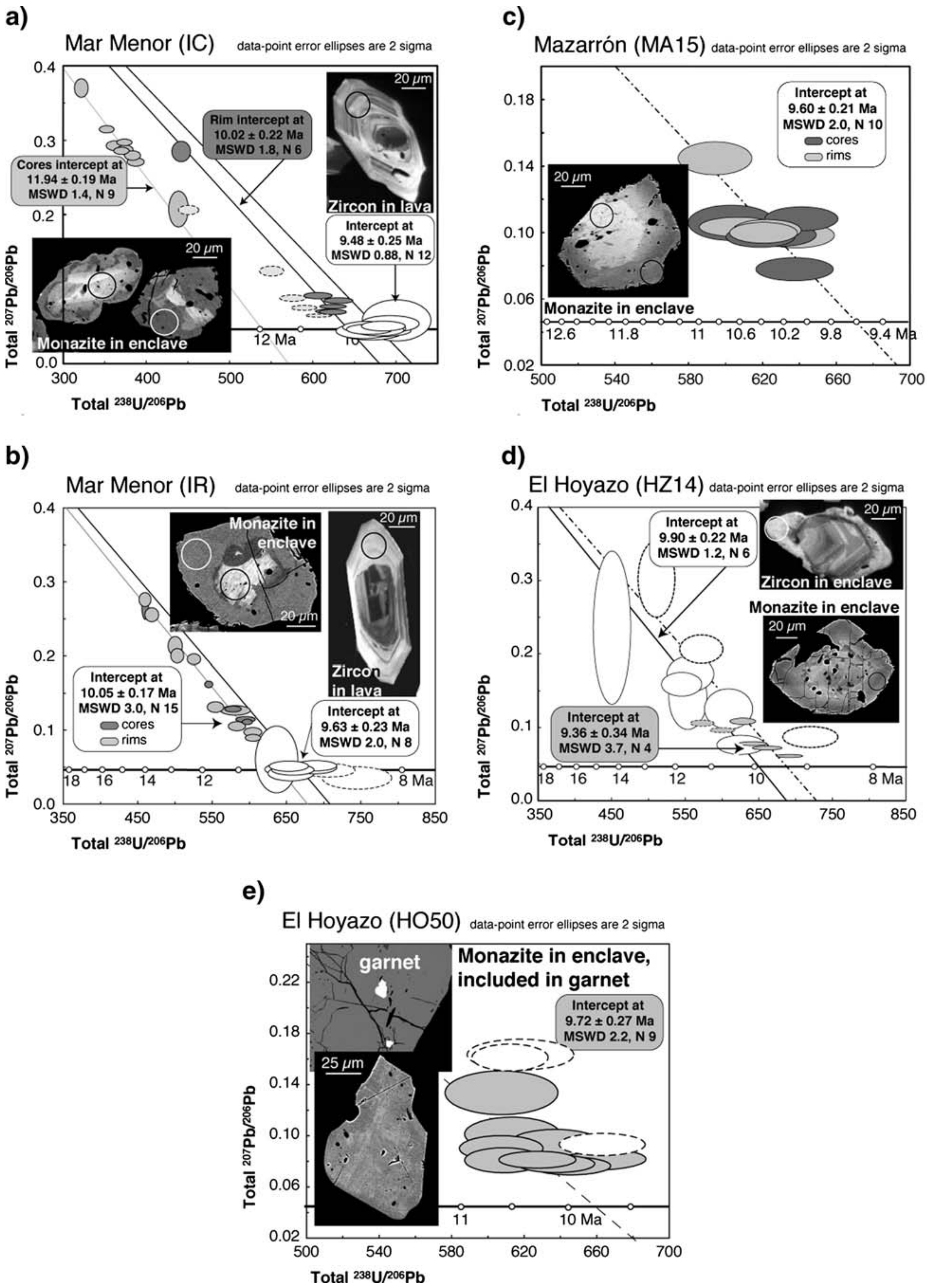
a)
Mar Menor (IC) data-point error ellipses are 2 sigma
Rim intercept at 10.02 ± 0.22 Ma MSWD 1.8, N 6
Cores intercept at 11.94 ± 0.19 Ma MSWD 1.4, N 9
Zircon in lava
Intercept at 9.48 ± 0.25 Ma MSWD 0.88, N 12
Monazite in enclave
12 Ma
Total 238U/206Pb
Total 207Pb/206Pb
c)
Mazarrón (MA15) data-point error ellipses are 2 sigma
Intercept at 9.60 ± 0.21 Ma MSWD 2.0, N 10
cores
rims
Monazite in enclave
12.6 11.8 11 10.6 10.2 9.8 9.4 Ma
b)
Mar Menor (IR) data-point error ellipses are 2 sigma
Monazite in enclave
Zircon in lava
Intercept at 10.05 ± 0.17 Ma MSWD 3.0, N 15
cores
rims
Intercept at 9.63 ± 0.23 Ma MSWD 2.0, N 8
18 16 14 12 8 Ma
d)
El Hoyazo (HZ14) data-point error ellipses are 2 sigma
Intercept at 9.90 ± 0.22 Ma MSWD 1.2, N 6
Zircon in enclave
Monazite in enclave
Intercept at 9.36 ± 0.34 Ma MSWD 3.7, N 4
18 16 14 12 10 8 Ma
e)
El Hoyazo (HO50) data-point error ellipses are 2 sigma
garnet
Monazite in enclave, included in garnet
Intercept at 9.72 ± 0.27 Ma MSWD 2.2, N 9
11 10 Ma

within the same error and define an age of 9.60 ± 0.21 Ma (Fig. 8c). This age is only marginally older than monazite from another enclave dated at 9.13 ± 0.18 Ma (Cesare et al. 2003b) and within error of the Mazarrón lava dated via U–Pb on zircon at 9.06 ± 0.53 Ma (Cesare et al. 2003b).

At El Hoyazo, a few monazite crystals were recovered from the small Spl-Crd-type enclave HZ14. They display limited zoning and yielded a poor age estimate of 9.36 ± 0.34 Ma out of only four analyses. Two other analyses with high common Pb yielded statistically older ages (10–10.5 Ma), which significance remains uncertain and could not be investigated due to the limited number of monazite recovered. The same enclave contains small zircon with detrital cores and rare unzoned overgrowths. Of the few overgrowths that could be analysed, six define a regression line with intercept at 9.90 ± 0.22 Ma (Fig. 8d), whereas three analyses that are either discordant or with high common Pb are excluded from the age calculation. Both zircon and monazite ages coincide within error with those from the Bt-Grt-Sil-type enclave dated by Cesare et al. (2003b). Garnet crystals extracted from enclave HO50 contains zircon similar to what previously described for El Hoyazo enclaves (Cesare et al. 2003b). The zircons have visible detrital cores and overgrowths (Fig. 7), which however are too small to be analysed without contamination from cores or surrounding garnet. Conversely, the monazite included in garnet from sample HO50 was successfully analysed in situ. If the 12 analyses are pooled together they show excessive scatter (9.55 ± 0.23 Ma, MSWD 5.6). When the three youngest analyses that have either high common Pb or are discordant are excluded, a better age constrain of 9.72 ± 0.27 Ma (MSWD 2.2) is obtained (Fig. 8e). Notably, monazite does not show significant zoning in BSE, neither systematic age variation from core to rim of the host garnet.

Discussion

Significance of ages and age differences

In order to interpret properly the geochronological results in terms of geodynamic and magmatologic implications a preliminary discussion of the significance of zircon and monazite ages is required. For the lavas, it is reasonable to assume that, given rapid cooling, the crystallization age of zircon with magmatic features (shape, zoning and Th–U composition) represents magma emplacement via volcanic extrusion. Pre-eruption zircon growth has been documented for periods of 0.03–0.25 Ma (e.g. Simon et al. 2008), which are close or below the error on our age estimates and thus do not affect our interpretation.

However, for the metapelitic enclaves this interpretation is more complex. Monazite or zircon will crystallize in a partially melted rock when the melt reaches saturation for P + REE or Zr, respectively. In metasedimentary anatectic rocks, this is commonly expected to occur early in the cooling path (Rubatto et al. 2006; Kelsey et al. 2008), but variations may occur according to local melt composition and degree of melting. In addition, zircon and monazite crystallization may also not be coeval within a rock (Rubatto et al. 2006; Kelsey et al. 2008). In the enclaves from El Hoyazo and Mazarrón, however, both monazite with melt inclusions (Figs. 4, 5) and zircon with euhedral overgrowths (Fig. 7) are observed not only in the rock matrix, but also within garnet. This suggest that garnet growth occurred after anatectic monazite and zircon had crystallized and thus these accessory minerals formed early in the melting process. An alternative interpretation is that growth of garnet and monazite was coeval to that of garnet and very fast, occurring in a time interval shorter than the analytical uncertainty, so that no age differences can be detected. Either way, since garnet contains also melt inclusions (Acosta-Vigil et al. 2007) in addition to zircon and monazite, we interpret monazite and zircon ages as dating the oldest melting event in the enclaves, i.e. the anatexis producing the Bt-Grt-Sil main assemblage (Cesare 2000). At Mar Menor, monazite in one enclave yielded multiple ages. Since monazites have melt inclusions (Fig. 8a), we interpret the older age of 11.94 Ma as evidence of an earlier melting event.

Since we are dating on one hand the production of anatectic magmas (with enclaves), and on the other their extrusion after contamination by mafic mantle melts (with lavas), the new ages allow the establishment of the overall chronological evolution of crustal anatexis and HKCA volcanism beneath the NVP. In turn, the age difference between enclaves and lavas in each locality is a measure of the delay between production at depth and extrusion at surface of crustally-derived melts, provided no previous eruption occurred, i.e. a measure of the time of residence of anatectic magmas within the crust. These interpretations rest on the assumption that there is no residence time for zircon, i.e. that zircon crystallizes in the lavas at the time of their extrusion. The validity of this assumption can be tested by cross-checking SHRIMP zircon ages with Ar/Ar ages from biotite in lavas: the data available in the literature suggest that SHRIMP and Ar/Ar ages overlap within error. Therefore, there is no evidence, at the present degree of uncertainty, of a prolonged residence of zircon in the lava prior to extrusion.

One might question if the lavas really represent the (contaminated) anatectic melts produced by the anatexis of enclaves, i.e. if enclaves are actually restite to the lavas (Vernon 2007). Felsic lavas, in fact, may include enclaves that represent restites of earlier (unrelated) partial melting events, as well as completely extraneous rock fragments. A definitive, positive, answer to this problem is probably impossible to give, as even in the case of perfect geochemical compatibility between lava and enclaves, the magmas might have been produced by the melting of a different, but geochemically analogue, source. Despite this unavoidable uncertainty, some important geological constraints need to be recalled: crustal fragments are found only in HKCA lavas, of which they represent a voluminous fraction; the crustal material is not heterogeneous but can be attributed to a few main rock types at each locality, and these are the types that have been dated; the enclaves have a residual composition that indicates very large (up to 50 wt.%) degrees of melting; there is ample evidence of syn-anatectic deformation attesting for a regional-scale anatectic event; there are no other felsic lavas of proposed anatectic origin outcropping in the region.

In summary we conclude that there is indeed an important link between HKCA lavas and the crustal enclaves, and that this link may be genetic. Furthermore, it should be emphasised that regardless of the presence or absence of a genetic link, the approach of this work, its conclusions and implications, are not invalidated, because in any case we are dating crustal melting with enclaves and felsic volcanism with lavas.

Production–extrusion delays

The geochronological results from this study are visualized in Fig. 9 together with additional data from Zeck and Williams (2002) and Cesare et al. (2003b). This summary allows distinguishing between the process of crustal melting at depth as recorded by mineral ages in the enclaves, and that of volcanic extrusion recorded by mineral ages in the lavas. In most geological occurrences, such a distinction is difficult or impossible to make, because one of the two processes cannot be dated. Extrusions are dated in volcanic rocks where data from the source are often lacking; crustal anatexis is dated in granulites and migmatites from which the magmas have escaped to an often unknown destination. And even if the timing of eruption and crustal melting can be obtained, in older terranes they could be irresolvable with modern dating techniques.

It is apparent from Fig. 9 that for the crustally derived HKCA magmas of the NVP the processes of production and extrusion do not always coincide in time, and that important delays may occur in between.

At Mar Menor, volcanism postdates crustal melting of 0.42 ± 0.13 m.y. (Isla Redondela) to 0.54 ± 0.14 m.y. (Isla del Ciervo). This time gap is even larger (2.46 ± 0.14 m.y.) if the age of 11.94 ± 0.19 Ma given by

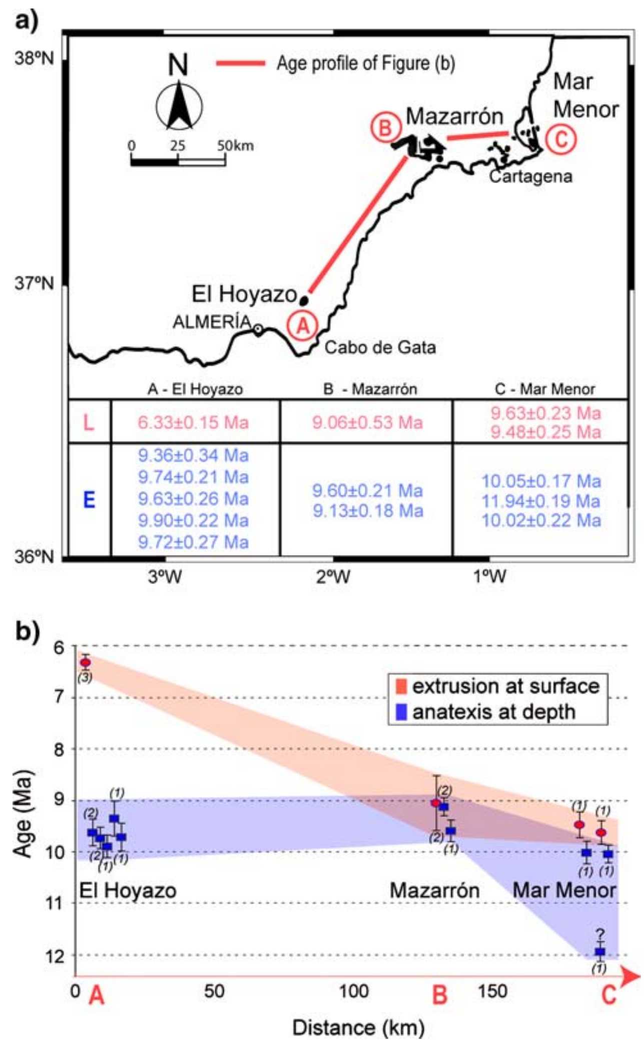

Fig. 9 **a** Summary of SHRIMP ages from crustal enclaves (*E*) and their high-K calc-alkaline lava hosts (*L*). **b** Distribution of SHRIMP ages from crustal enclaves (*blue*) and their high-K calc-alkaline volcanic hosts (*pink*) along El Hoyazo–Mazarrón–Mar Menor transect (*A–B–C* profile in **a**). *1* this work; *2* Cesare et al. 2003b; *3* Zeck and Williams (2002)

the monazite core in sample IC10 represents initial melting.

At Mazarrón, the new data of 9.60 ± 0.21 Ma from the enclave, although older than that determined in another sample, is not sufficiently different from the age of the lava (9.06 ± 0.53, Cesare et al. 2003b) to claim a delay between anatexis and eruption. Therefore at Mazarrón anatectic melts appear to have resided at depth for the shortest period. In this locality, the monazite ages obtained from different enclaves (9.60 ± 0.22 this work and 9.13 ± 0.18 Ma, Cesare et al. 2003b) are significantly apart (0.47 ± 0.13 m.y.) to support separate events or a prolonged history of partial melting at depth.

At El Hoyazo, the age of 9.36 Ma (monazite) and 9.90 Ma (zircon) from the Spl-Crd-type enclave and that from the monazite included in garnet in HO50 (9.72 Ma) confirm that after crustal melting the enclaves and anatectic magmas resided at the base of the crust for >3 m.y. before erupting (Zeck and Williams 2002; Cesare et al. 2003b). We propose that, during this time, the rocks resided at high-temperature conditions (>800°C). Alternatively, rapid heating and partial melting at >9 Ma was followed by cooling, crystallization and re-melting at c. 6 Ma. This second scenario seems unlikely in the light of the available data, including the absence of the typical microstructures of rapidly heated pyrometamorphic xenoliths (e.g. Holness 2008), Sm/Nd isotopic data pointing to quasi-equilibrium among minerals and glass within enclaves (Perini et al. 2008), abundance and fresh glass in the enclaves, and geodynamic interpretation (the regional scale of crustal melting beneath the NVP is inconsistent with a transient thermal pulse).

The fact that anatectic magmas may reside at depth, prior to extrusion, for periods in excess of 3 m.y., affects important geochemical issues, such as equilibrium versus disequilibrium between melts and their sources (e.g. Tommasini and Davies 1997; Perini et al. 2008). Long delays are to be expected also in plutonic settings, where anatectic granites may crystallize later than when the magmas have been produced (Barbero and Villaseca 1992; Barbero et al. 1995). The m.y.-long times of residence discussed here, which refer to the ponding of magmas at the base of, or in the deep crust, should not be compared with the residence times of felsic magmas often discussed in the literature. The latter, in fact, generally refer to the stagnation of magma in upper crustal, shallow chambers, where residence is much shorter and exceptionally long times are in the order of 10^5 years (e.g. Reid et al. 1997; Davies and Halliday 1998; Heath et al. 1998).

Origin of garnet in the Bt-Grt-Sil enclaves from El Hoyazo

Garnet from Bt-Grt-Sil enclaves has been interpreted as the peritectic product of a melting reaction based on the common occurrence of glass inclusions (e.g. Acosta-Vigil et al. 2007) with zonal arrangement (Sobolev and Kostyuk 1975), and on complementary petrologic data (summarised by Cesare 2008). In this perspective, it has been postulated that garnet crystals growing in the presence of melt were able to trap droplets of liquid, now observed as melt inclusions (Cesare and Maineri 1999). This view has been challenged by Vernon (2007) who proposed that garnet existed prior to melting and that melt inclusions formed by the melting of solid phases included in it.

The age of monazite crystals that occur within garnet extracted from sample HO50, overlap within error with those of monazite occurring in the rock matrix of similar samples (e.g. HO02 and HO33; Cesare et al. 2003b). Dated monazite occurs in all textural positions (core, intermediate, rim) within garnets cut on equatorial sections, without age younging toward the rims. Owing to the occurrence of melt inclusions within both monazite (Figs. 4, 5) and garnet, these data indicate: (1) that monazite grew in the presence of melt at 9.72 ± 0.27 Ma; (2) that garnet grew in the presence of melt *after* or during (see above) monazite growth. Therefore garnet is 9.72 ± 0.27 Ma or younger in age, and syn-anatectic.

This independent age constraint, that adds to the discussion on the origin of melt inclusions (Cesare 2008), is in favour of a peritectic origin of garnet in the Bt-Grt-Sil enclaves of El Hoyazo, and against the proposition that garnet existed prior to melting (Vernon 2007).

Regional implications

The comprehensive dataset summarised in Fig. 9 shows that an important event of crustal melting took place beneath the Alborán Domain in the time interval 12–9 Ma, a period when only calc-alkaline magmatism was so far considered to be occurring (Comas et al. 1999; Zeck et al. 2000). In fact, current models for the age of crustal melting in the region, based on volcanic extrusions, report much younger ages of c. 6 Ma for anatectic rocks from SE Spain (Duggen et al. 2004). The new age constraints are thus an important contribution to the geochronological and magmatogenetic evolution of this part of the western Mediterranean. At Mazarrón and Mar Menor extrusion followed immediately or shortly after magma production. Conversely, at El Hoyazo after crustal melting at >9 Ma, anatectic magmas resided at depth until final extrusion at c. 6 Ma. Extrusions were probably triggered by the emplacement of hot mafic magmas, which interacted and mixed with the crustal melts, and favoured by fault systems active in that period (De Larouziere et al. 1988).

A genetic relationship between the Grt-Crd-bearing lavas and the lamproites of SE Spain has been previously proposed in terms of crustal contamination of mantle-derived lamproitic magmas (Duggen et al. 2005). Our results constrain the crustal melting to the minimum period of 12–9 Ma, well before the onset of lamproitic volcanism at 8–5 Ma (Duggen et al. 2005, 2008). This age difference implies that, if the genetic relationship is acceptable, some of the lamproitic magmas were present at depth a few million years before eruption, in the period when calc-alkaline magmas erupted in the NVP.

In addition, the new data clarify the age of extrusion of volcanics with crustal components from Mar Menor. Our ages of 9.5–9.6 Ma for the Mar Menor lavas contrasts with the 18.5 Ma Ar/Ar age obtained by Duggen et al. (2004) on feldspar from similar volcanics. Interpretation of the latter as representative of the crustal melting event is problematic, as our new data indicate that the anatectic melts at Mar Menor formed in the period 10–12 Ma.

Geodynamic pitfalls

Along with the bearings on the chronology of magmatism in the Alborán Domain, this work has a wider, methodological implication, i.e., that ages of extrusion do not necessarily reflect the timing of melting occurring at the magma source. On one hand, there is a variable delay (in this study up to >3 m.y.) between magma production and lava extrusion. On the other hand, the younging of volcanism at the surface towards SW (9.5 to 9.1 to 6.3 Ma from Mar Menor to El Hoyazo) is not mimicked by a similar pattern in the magma production at depth, because anatexis at El Hoyazo occurred earlier than at Mazarrón (9.9 vs. 9.6 Ma; Fig. 9). Unlike the fictive trend provided by volcanic ages (e.g. Gill et al. 2004; Duggen et al. 2005), the age of crustal melting beneath the NVP does not provide further support to models of westward migration of magmatism. At present, when dealing with the time/space reconstructions of volcanism in the NVP, it is safer to state that the HKCA volcanic rocks were produced in the same period throughout the area.

The example of the NVP shows that the common practice of basing geodynamic models on ages of volcanic extrusions (e.g. Christiansen et al. 2002; Jordan et al. 2004) should be used with caution. This practice may be reasonable for mantle magmas rapidly ascending through thin oceanic lithosphere, i.e. for detecting plate movements and velocities above oceanic hot spots (Sharp and Clague 2006). It can also be reliable where large datasets of extrusion ages from felsic volcanics provide a consistent time/space pattern over large areas. This approach has been successful in constraining, for example, the southward "sweep" of Tertiary volcanism in the northern Basin and Range Province (e.g. Best and Christiansen 1991). However, where cold and viscous anatectic magmas have to ascend through a relatively thick crust, and where data are limited, as in the NVP of SE Spain, the age of volcanic rocks may provide misleading geographic polarities and time constraints on the processes at depth.

Conclusions

The eruption of Grt-Crd-bearing volcanics at Mar Menor occurred at 9.5 ± 0.2 Ma, later than previously proposed. In this and other localities along the NVP, crustal anatexis took place significantly earlier than the extrusion of magmas with crustal components. Overall, crustal anatexis beneath the NVP of SE Spain spans at least the time interval between 12 and 9 Ma, whereas extrusion of the crustally derived HKCA volcanic rocks is delayed at 9–6 Ma.

These results show that crustal melting is significantly older than commonly assumed, and that a re-assessment of the chronology of magmatism in the NVP is required.

The assumption that volcanism at the Earth's surface is synchronous with magma generation at depth is not necessarily correct. Our results highlight the potential pitfalls of basing geodynamic models and chronological reconstructions on extrusion ages.

Acknowledgments We wish to thank Antonio Acosta-Vigil, I. Buick, J.M. Fernandez-Soler and J. Hermann for discussion, A. Patiño-Douce and B. Clarke for reviewing an earlier version of the manuscript, and two anonymous reviewers for their helpful comments. The Electron Microscopy Unit at ANU is thanked for access to the SEM facilities. We acknowledge the financial support of Ministero dell'Università e della Ricerca (PRIN 2005-047810) and Consiglio Nazionale delle Ricerche (Euromargins ESF Eurocore) to BC, of CGL2006-04440 (MEC) and RNM-0145 (Junta de Andalucía) to MTG-P, and of the Australian Research Council to DR.

References

Acosta-Vigil A, Cesare B, London D, Morgan GBVI (2007) Microstructures and composition of melt inclusions in a crustal anatectic environment: the metapelitic enclaves within El Hoyazo dacites, SE Spain. Chem Geol 237:450–465. doi:10.1016/j.chemgeo.2006.07.014

Aleinikoff JN, Schenck WS, Plank MO, Srogi L, Fanning CM, Kamo SL, Howell B (2007) Deciphering igneous and metamorphic events in high-grade rocks of the Wilmington Complex, Delaware: Morphology, cathodoluminescence and backscattered electron zoning, and SHRIMP U-Pb geochronology of zircon and monazite. Geol Soc Am Bull 118:39–64. doi:10.1130/B25659.1

Alvarez-Valero AM, Kriegsman LM (2007) Crustal thinning and mafic underplating beneath the Neogene Volcanic Province (Betic Cordillera, SE Spain): evidence from crustal xenoliths. Terra Nova 19:266–271. doi:10.1111/j.1365-3121.2007.00745.x

Álvarez-Valero AM, Kriegsman LM (2008) Partial crustal melting beneath the Betic Cordillera (SE Spain): the case study of Mar Menor volcanic suite. Lithos 101:379–396

Alvarez-Valero AM, Cesare B, Kriegsman LM (2005) Formation of elliptical garnets in a metapelitic enclave by meltassisted dissolution and reprecipitation. J Metamorph Geol 23:65–74

Alvarez-Valero AM, Cesare B, Kriegsman LM (2007) Formation of spinel-cordierite-feldspar-glass coronas after garnet in metapelitic xenoliths: reaction modelling and geodynamic implications. J Metamorph Geol 25:305–320. doi:10.1111/j.1525-1314.2007.00690.x

Barbero L, Villaseca C (1992) The Layos granite, Hercynian Complex of Toledo (Spain): an example of parauthoctonous restite-rich granite in a granulite area. Trans R Soc Edinb Earth Sci 83:127–138

Barbero L, Villaseca C, Rogers G, Brown PE (1995) Geochemical and isotopic disequilibrium in crustal melting: an insight from the anatectic granitoids from Toledo, Spain. J Geophys Res 100:15745–15765. doi:10.1029/95JB00036

Bellon H, Bordet P, Montenat C (1983) Chronologie du magmatisme néogène des Cordillères bétiques (Espagne méridionale). Bull Soc Geol Fr 25:205–217

Benito R, Lopez-Ruiz J, Cebriá JM, Hertogen J, Doblas M, Oyarzun R, Demaiffe D (1999) Sr and O isotope constraints on source and

crustal contamination in the high-K calc-alkaline and shoshonitic neogene volcanic rocks of SE Spain. Lithos 46:773–802. doi:10.1016/S0024-4937(99)00003-1
Best MG, Christiansen EH (1991) Limited extension during peak Tertiary volcanism, Great Basin of Nevada and Utah. J Geophys Res 96:13509–13528
Black LP, Kamo SL, Allen CM, Aleinikoff JM, Davis DW, Korsch RJ, Foudoulis C (2003) TEMORA 1: a new zircon standard for Phanerozoic U–Pb geochronology. Chem Geol 200:155–170
Cesare B (2000) Incongruent melting of biotite to spinel in a quartz-free restite at El Joyazo (SE Spain): textures and reaction characterization. Contrib Mineral Petrol 139:273–284. doi:10.1007/s004100000137
Cesare B (2008) Crustal melting: working with enclaves. In: Sawyer EW, Brown M (eds) Working with migmatites. Mineral Assoc Canada Short Course, vol 38, pp 37–55
Cesare B, Gomez-Pugnaire MT (2001) Crustal melting in the Alborán domain: constraints from the xenoliths of the Neogene Volcanic Province. Phys Chem Earth 26:255–260. doi:10.1016/S1464-1895(01)00053-9
Cesare B, Maineri C (1999) Fluid-present anatexis of metapelites at El Joyazo (SE Spain): constraints from raman spectroscopy of graphite. Contrib Mineral Petrol 135:41–52. doi:10.1007/s004100050496
Cesare B, Salvioli Mariani E, Venturelli G (1997) Crustal anatexis and melt extraction in the restitic xenoliths at El Hoyazo (SE Spain). Mineral Mag 61:15–27. doi:10.1180/minmag.1997.061.404.03
Cesare B, Gomez-Pugnaire MT, Sanchez-Navas A, Grobety B (2002) Andalusite—sillimanite replacement (Mazarrón—SE Spain): microstructural and TEM study. Am Mineral 87:433–444
Cesare B, Cruciani G, Russo U (2003a) Hydrogen deficiency in Ti-rich biotite from anatectic metapelites (El Joyazo—SE Spain): crystal-chemical aspects and implications for high-temperature petrogenesis. Am Mineral 88:583–595
Cesare B, Gomez-Pugnaire MT, Rubatto D (2003b) Residence time of S-type anatectic magmas beneath the Neogene Volcanic Province of SE Spain: a zircon and monazite SHRIMP study. Contrib Mineral Petrol 146:28–43. doi:10.1007/s00410-003-0490-x
Cesare B, Marchesi C, Hermann J, Gomez-Pugnaire MT (2003c) Primary melt inclusions in andalusite from anatectic graphitic metapelites: Implications for the position of the Al_2SiO_5 triple point. Geology 31:573–576. doi :10.1130/0091-7613(2003)0310573:PMIIAF2.0.CO;2
Cesare B, Meli S, Nodari L, Russo U (2005) Fe^{3+} reduction during biotite melting in graphitic metapelites: another origin of CO2 in granulites. Contrib Mineral Petrol 149:129–140. doi:10.1007/s00410-004-0646-3
Cesare B, Maineri C, Baron Toaldo A, Pedron D, Acosta-Vigil A (2007) Immiscibility between carbonic fluids and granitic melts during crustal anatexis: a fluid and melt inclusion study in the enclaves of the Neogene Volcanic Province of SE Spain. Chem Geol 237:433–449. doi:10.1016/j.chemgeo.2006.07.013
Christiansen RL, Foulger GR, Evans JR (2002) Upper-mantle origin of the Yellowstone hotspot. Geol Soc Am Bull 114:245–1256. doi :10.1130/0016-7606(2002)1141245:UMOOTY2.0.CO;2
Clemens JD (2003) S-type granitic magmas—petrogenetic issues, models and evidence. Earth Sci Rev 61:1–18. doi:10.1016/S0012-8252(02)00107-1
Clemens JD, Droop GTR (1998) Fluids, P-T paths and the fates of anatectic melts in the Earth's Crust. Lithos 44:21–36. doi:10.1016/S0024-4937(98)00020-6
Comas MC, Zahn R, Klaus A, Aubourg C, Bernasconi SM, Belanger PE, Cornell W, de Kaenel EP, de Larouzière FD, Doglioni C, Doose H, Fukusawa H, Hobart M, Iaccarino SM, Ippach P, Marsaglia K, Meyers P, Murat A, O'Sullivan GM, Platt JP, Prasad M, Siesser WG, Skilbeck CG, Soto JI, Tandon K, Torii M, Tribble JS, Wilkens RH (1996) In: Proceedings of the ocean drilling program, Initial Reports 161, Ocean Drilling Program, College Station, TX
Comas MC, Platt JP, Soto JI, Watts AB (1999) The origin and tectonic history of the Alborán Basin: insights from Leg 161. In: Zahn R, Comas MC, Klaus A (eds) Proceedings of the ocean drilling program, scientific results, vol 161, pp 555–579
Davies GR, Halliday AN (1998) Development of the Long Valley rhyolitic magma system: strontium and neodymium isotope evidence from glasses and individual phenocrysts. Geochim Cosmochim Acta 62:3561–3574. doi:10.1016/S0016-7037(98)00247-6
De Larouziere FD, Bolze J, Bordet P, Hernandez J, Montenat C, Ott d'Estevou P (1988) The betic segment of the lithospheric Trans-Alborán shear zone during the late Miocene. Tectonophysics 152:41–52. doi:10.1016/0040-1951(88)90028-5
De Larouziere FM, Ott d'Estevou P (1990) Les bassins d'Hinojar et Mazarrón. In: Montenat C (ed) Les bassins néogenes du Domaine Bétique Oriental (Espagne). Documents et Travaux IGAL, vol 12–13, pp 207–220
Duggen S, Hoernle K, van den Bogaard P, Harris C (2004) Magmatic evolution of the Alborán region: the role of subduction in forming the western Mediterranean and causing the Messinian Salinity Crisis. Earth Planet Sci Lett 218:91–108. doi:10.1016/S0012-821X(03)00632-0
Duggen S, Hoernle K, van den Bogaard P, Garbe-Schönberg D (2005) Post-collisional transition from subduction- to intraplate-type magmatism in the westernmost Mediterranean: evidence for continental-edge delamination of subcontinental lithosphere. J Petrol 46:1155–1201. doi:10.1093/petrology/egi013
Duggen S, Hoernle K, Klügel A, Geldmacher J, Thirlwall M, Hauff F, Lowry D, Oates N (2008) Geochemical zonation of teh Miocene Alborán Basin volcanism (westernmost Mediterranean) geodynamic implications. Contrib Mineral Petrol (in press)
Fernández-Soler JM (1996) El volcanismo calco-alcalino en el parque natural de Cabo de Gata-Níjar (Almería). Estudio Volcanológico y Petrológico. Soc Almeriense Hist Natural. Monografias Medio Nat 2:1–295
Fernández-Soler JM, Acosta-Vigil A, Gómez-Pugnaire MT, Comas MC (2007) Magma mixing in El Hoyazo volcanics, Betic Cordilleras (SE Spain). Geophys Res Abstr 9:04202
Ferri F, Burlini L, Cesare B, Sassi R (2007) Seismic properties of lower crustal xenoliths from El Hoyazo (SE Spain): experimental evidence up to partial melting. Earth Planet Sci Lett 253:239–253. doi:10.1016/j.epsl.2006.10.027
García-Dueñas V, Balaná JC, Martínez-Martínez JM (1992) Miocene extensional detachments in the outcropping basement of the northern Alborán basin (Betics) and their tectonic implications. Geo-Mar Lett 12:88–95. doi:10.1007/BF02084917
Gill RCO, Aparicio A, El Azouzzi M, Hernández J, Thirlwall MF, Bourgois J, Marriner GF (2004) Depleted arc volcanism in the Alborán Sea and shoshonitic volcanism in Morocco: geochemical and isotopic constraints on Neogene tectonic processes. Lithos 78:363–388. doi:10.1016/j.lithos.2004.07.002
Gracia E, Pallas R, Soto JI, Comas M, Moreno X, Masana E, Santanach P, Diez S, Garcia M, Danobeitia J, Scientific Party HITS (2006) Active faulting offshore SE Spain (Alboran Sea): implications for earthquake hazard assessment in the Southern Iberian Margin. Earth Planet Sci Lett 241:734–749. doi:10.1016/j.epsl.2005.11.009
Gueguen E, Doglioni C, Fernandez M (1998) On the post-25 Ma geodynamic evolution of the western Mediterranean. Tectonophysics 298:259–269
Heath E, Turner SP, Macdonald R, Hawkesworth CJ, van Calsteren P (1998) Long magma residence times at an island arc volcano

(Soufriere, St. Vincent) in the Lesser Antilles: evidence from ^{238}U–^{230}Th isochron dating. Earth Planet Sci Lett 160:4–63. doi:10.1016/S0012-821X(98)00084-3
Holness MB (2008) Decoding migmatite microstructures. In: Sawyer EW, Brown M (eds) Working with migmatites. Mineral Assoc Canada Short Course, vol 38, pp 57–76
Jordan BT, Grunder AL, Duncan RA, Deino AL (2004) Geochronology of age-progressive volcanism of the Oregon High Lava Plains: implications for the plume interpretation of Yellowstone. J Geophys Res 109:B10202. doi:10.1029/2003JB002776
Kelsey DE, Clark C, Hand M (2008) Thermobarometric modelling of zircon and monazite growth in melt-bearing systems: examples using model metapelitic and metapsammitic granulites. J Metamorph Geol 26:199–212. doi:10.1111/j.1525-1314.2007.00757.x
Kretz R (1983) Symbols for rock-forming minerals. Am Mineral 68:277–279
López Ruiz J, Rodríguez Badiola E (1980) La región volcánica neógena del sureste de España. Est Geol 36:5–63
Ludwig KR (2003) Isoplot/Ex version 3.0. A geochronological toolkit for Microsoft Excel. 1a: Berkeley Geochronological Centre Spec Pub, Berkeley
Pallister JS, Hoblitt RP, Crandell DR, Mullineaux DR (1992) Mount St. Helens a decade after the 1980 eruptions: magmatic models, chemical cycles, and revised hazards assessment. Bull Volcanol 54:126–146. doi:10.1007/BF00278003
Perini G, Cesare B, Gómez-Pugnaire MT Ghezzi, Tommasini S (2008) Armouring effect in decoupling Sr-Nd isotopes during disequilibrium crustal melting: the case study of frozen migmatites from El Hoyazo and Mazarrón, SE Spain. Eur J Mineral (in press)
Petford N, Cruden AR, McCaffrey KJW, Vigneresse JL (2000) Granite magma formation, transport and emplacement in the Earth's crust. Nature 408:669–673. doi:10.1038/35047000
Platt JP, Whitehouse MJ, Kelley SP, Carter A, Hollick L (2003) Simultaneous extensional exhumation across the Alborán basin: Implications for the causes of late-orogenic extension. Geology 31:251–254. doi :10.1130/0091-7613(2003)0310251:SEEATA2.0.CO;2
Reid MR, Coath CD, Harrison TM, McKeegan KD (1997) Prolonged residence times for the youngest rhyolites associated with Long Valley Caldera: ^{230} Th-^{238} U ion microprobe dating of young zircons. Earth Planet Sci Lett 150:327–339. doi:10.1016/S0012-821X(97)00077-0
Rubatto D, Hermann J, Buick IS (2006) Temperature and bulk composition control on the growth of monazite and zircon during low-pressure anatexis (Mount Stafford, central Australia). J Petrol 47:1973–1996. doi:10.1093/petrology/egl033
Sharp WD, Clague DA (2006) 50-Ma initiation of Hawaiian-Emperor Bend records major change in Pacific Plate motion. Science 313:1281–1284. doi:10.1126/science.1128489
Simon JI, Renne PR, Mundil R (2008) Implications of pre-eruptive magmatic histories of zircons for U–Pb geochronology of silicic extrusions. Earth Planet Sci Lett 266:182–194. doi:10.1016/j.epsl.2007.11.014
Sobolev VS, Kostyuk VP (1975) Magmatic crystallization based on a study of melt inclusions. Fluid Incl Res 9:182–253 (translated from original pubblication in Russian)
Stacey JS, Kramers JD (1975) Approximation of terrestrial lead evolution by a two-stage model. Earth Planet Sci Lett 26:207–221. doi:10.1016/0012-821X(75)90088-6
Tommasini S, Davies GR (1997) Isotope disequilibrium during anatexis: a case study of contact melting, Sierra Nevada, CA. Earth Planet Sci Lett 148:273–285. doi:10.1016/S0012-821X(97)00031-9
Torne M, Fernández M, Comas MC, Soto JI (2000) Lithospheric structure beneath the Alborán Basin: results from 3D Gravity modeling and tectonic relevance. J Geophys Res 105:3209–3228. doi:10.1029/1999JB900281
Turner SP, Platt JP, George RMM, Kelley SP, Pearson DG, Nowell GM (1999) Magmatism associated with orogenic collapse of the Betic-Alborán Domain, SE Spain. J Petrol 40:1011–1036. doi:10.1093/petrology/40.6.1011
Venturelli G, Capedri S, Di Battistini G, Crawford A, Kogarko LN, Celestini S (1984) The ultrapotassic rocks from southeastern Spain. Lithos 17:37–54. doi:10.1016/0024-4937(84)90005-7
Vernon RH (2007) Problems in identifying restite in S-type granites of southeastern Australia, with speculations on sources of magma and enclaves. Can Mineral 45:147–178. doi:10.2113/gscanmin.45.1.147
Williams IS (1998) U-Th–Pb geochronology by ion microprobe. In: McKibben MA, Shanks WC III, Ridley WI (eds) Applications of microanalytical techniques to understanding mineralizing processes. Reviews in economic geology, pp 1–35
Zeck HP (1970) An erupted migmatite from Cerro del Hoyazo, SE Spain. Contrib Mineral Petrol 26:225–246. doi:10.1007/BF00373202
Zeck HP (1992) Restite-melt and mafic-felsic magma mingling in an S-type dacite, Cerro del Hoyazo, southeastern Spain. Trans R Soc Edinb Earth Sci 83:139–144
Zeck HP, Williams IS (2002) Inherited and magmatic zircon from Neogene Hoyazo cordierite dacite, SE Spain–Anatectic source rock provenance and magmatic evolution. J Petrol 43:1089–1104. doi:10.1093/petrology/43.6.1089
Zeck HP, Kristensen AB, Williams IS (1998) Post-collisional volcanism in a sinking slab setting—crustal anatectic origin of pyroxene-andesite magma, Caldear Volcanic Group, Neogene Alborán volcanic Province, southeastern Spain. Lithos 45:499–522. doi:10.1016/S0024-4937(98)00047-4
Zeck HP, Maluski H, Kristensen AB (2000) Revised geochronology of the Neogene calc-alkaline volcanic suite in Sierra de Gata, Alborán volcanic province, SE Spain. J Geol Soc 157:75–81